



Murdoch
UNIVERSITY

MURDOCH RESEARCH REPOSITORY

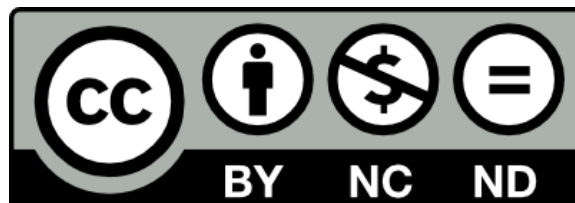
This is the author's final version of the work, as accepted for publication following peer review but without the publisher's layout or pagination.

The definitive version is available at

<http://dx.doi.org/10.1016/j.neuroscience.2016.08.030>

Tang, A.D., Hong, I., Boddington, L.J., Garrett, A.R., Etherington, S., Reynolds, J.N.J. and Rodger, J. (2016) Low-intensity repetitive magnetic stimulation lowers action potential threshold and increases spike firing in layer 5 pyramidal neurons in vitro. *Neuroscience*, 335 . pp. 64-71.

<http://researchrepository.murdoch.edu.au/33129/>



Copyright: © 2016 IBRO.

Please cite this article in press as: Tang AD et al. Low-intensity repetitive magnetic stimulation lowers action potential threshold and increases spike firing in layer 5 pyramidal neurons *in vitro*. *Neuroscience* (2016), <http://dx.doi.org/10.1016/j.neuroscience.2016.08.030>

Neuroscience xxx (2016) xxx–xxx

LOW-INTENSITY REPETITIVE MAGNETIC STIMULATION LOWERS ACTION POTENTIAL THRESHOLD AND INCREASES SPIKE FIRING IN LAYER 5 PYRAMIDAL NEURONS *IN VITRO*

ALEXANDER D. TANG,^{a,*} IVAN HONG,^b
LAURA J. BODDINGTON,^{c,d} ANDREW R. GARRETT,^a
SARAH ETHERINGTON,^b JOHN N. J. REYNOLDS^{c,d} AND
JENNIFER RODGER^a

^a *Experimental and Regenerative Neurosciences, School of Animal Biology, University of Western Australia, Perth, Australia*

^b *School of Veterinary and Life Sciences, Murdoch University, Perth, Australia*

^c *Brain Health Research Centre and Brain Research NZ Centre of Research Excellence, New Zealand*

^d *Department of Anatomy, University of Otago, Dunedin, New Zealand*

Abstract—Repetitive transcranial magnetic stimulation (rTMS) has become a popular method of modulating neural plasticity in humans. Clinically, rTMS is delivered at high intensities to modulate neuronal excitability. While the high-intensity magnetic field can be targeted to stimulate specific cortical regions, areas adjacent to the targeted area receive stimulation at a lower intensity and may contribute to the overall plasticity induced by rTMS. We have previously shown that low-intensity rTMS induces molecular and structural plasticity *in vivo*, but the effects on membrane properties and neural excitability have not been investigated. Here we investigated the acute effect of low-intensity repetitive magnetic stimulation (LI-rMS) on neuronal excitability and potential changes on the passive and active electrophysiological properties of layer 5 pyramidal neurons *in vitro*. Whole-cell current clamp recordings were made at baseline prior to subthreshold LI-rMS (600 pulses of iTBS, $n = 9$ cells from 7 animals) or sham ($n = 10$ cells from 9 animals), immediately after stimulation, as well as 10 and 20 min post-stimulation. Our results show that LI-rMS does not alter passive membrane properties (resting membrane potential and input resistance) but hyperpolarises action potential threshold and increases evoked spike-firing frequency. Increases in spike firing frequency were present throughout the 20 min post-stimulation whereas action potential (AP) threshold hyperpolarization was present immediately after stimulation and at 20 min post-stimulation. These results provide evidence that LI-rMS alters neuronal excitability of excitatory neurons. We suggest that regions outside the targeted region

of high-intensity rTMS are susceptible to neuromodulation and may contribute to rTMS-induced plasticity. © 2016 IBRO. Published by Elsevier Ltd. All rights reserved.

Key words: low-intensity rMS, action potential threshold, spike firing frequency, Intermittent Theta Burst Stimulation.

INTRODUCTION

Repetitive transcranial magnetic stimulation (rTMS) is a popular form of non-invasive brain stimulation used to induce neural plasticity in both clinical and non-clinical populations. rTMS delivers trains of magnetic fields over the scalp which in turn induce electrical currents in the underlying brain. The high-intensity magnetic fields delivered are of the same magnitude of MRI scanners ($> 1\text{T}$) (Ridding and Rothwell, 2007) and can be targeted to stimulate specific brain regions (e.g. motor cortex) and to alter neuronal excitability (e.g. corticospinal excitability). The onset of rTMS-induced changes in corticospinal excitability occurs immediately after stimulation and the effects persist for minutes to hours after stimulation (Huang et al., 2005; Ziemann et al., 2008; Wischnewski and Schutter, 2015). The mechanisms underlying rTMS neuromodulation are unclear, but are believed to involve changes in neuronal membrane properties (Hoppenrath et al., 2016), synaptic and non-synaptic mechanisms (Tang et al., 2015).

While specific regions can be targeted, such that the maximal current induced occurs at the targeted region, regions adjacent also receive stimulation with weaker induced electrical currents and the spread of electrical current from the targeted region (Wagner et al., 2009). The role of low-intensity stimulation in the overall rTMS-induced plasticity remains unclear but studies using extremely low magnetic fields ($\sim 0.002\text{T}$) have shown changes to neurophysiology (for a review see (Di Lazzaro et al., 2013)) and possibly to cortical excitatory neurotransmission (Capone et al., 2009). In mouse models, we have previously shown that low-intensity rTMS (0.01 T) induces molecular and functional plasticity (Rodger et al., 2012; Makowiecki et al., 2014).

Experimental models of repetitive magnetic stimulation (LI-rMS) using organotypic tissue cultures or brain slices from animals provide a useful adjunct to human studies as they allow direct measurement of

*Corresponding authors. Address: University of Western Australia, 35 Stirling Highway, Crawley 6009, Western Australia, Australia.

E-mail addresses: Alexander.Tang@research.uwa.edu.au (A.D. Tang), jennifer.rodger@uwa.edu.au (J. Rodger).

Abbreviations: ACSF, artificial cerebrospinal fluid; AHP, after hyperpolarization; AP, action potential; LI-rMS, low-intensity repetitive magnetic stimulation; RMP, resting membrane potential; rTMS, repetitive transcranial magnetic stimulation.

plasticity at the single-cell level and provide insights into the cellular changes occurring after rTMS (for a review see (Müller-Dahlhaus and Vlachos, 2013; Tang et al., 2015)). Single-cell electrophysiological studies on brain slices of rats that received high-intensity rTMS show changes in the resting membrane potential and evoked spike firing of layer 2/3 fast spiking interneurons two hours after stimulation (Hoppenrath et al., 2016). However the effects of LI-rMS on the electrophysiological properties of cortical excitatory neurons are unknown. To investigate these effects, we employed *in vitro* whole-cell patch clamp electrophysiology on layer 5 pyramidal neurons from mouse motor and somatosensory brain slices. We investigated both passive and active membrane properties and evoked spiking properties following LI-rMS or sham stimulation over a 20-min period post-stimulation. Our results show that LI-rMS does not alter passive membrane properties but increases neural excitability by inducing hyperpolarized action potential thresholds and increases the evoked spike firing rate.

EXPERIMENTAL PROCEDURES

Ethics approval

All procedures were approved by the University of Western Australia animal ethics committee (RA/3/100/1229) which is in accordance with the Australian code of practice for the care and use of animals for scientific purposes.

Slice preparation

C57Bl/6J mice (post-natal days 12–15, of either sex, $n = 11$) were acquired from the Animal Resource Centre (Murdoch, Australia). Juvenile animals were chosen due to the high quality and longevity of the slices that they provide. Mice were terminally anaesthetized with an intra-peritoneal injection of pentobarbitone (> 160 mg/kg) followed by rapid dissection of the brain. Acute brain slices (300 μ m thick) were prepared from the motor and somatosensory cortex. Coronal slices of cortex were prepared with a vibrating slicer (Campden Instruments 5000-mz) and ice-cold cutting solution comprising (mM) 125 NaCl, 3 KCl, 0.5 CaCl₂, 6 MgCl₂, 25 NaHCO₃, 1.25 NaH₂PO₄ and 10 glucose bubbled with carbogen (5% CO₂/95% O₂). Slices were kept at 35 °C for 1 h in a holding chamber containing carbogen-bubbled artificial CSF (artificial cerebrospinal fluid (ACSF), see below for composition), after which they were held at room temperature until required.

Electrophysiology

Slices received continuous perfusion (~ 1.5 mL/min) with ACSF comprising (mM) 125 NaCl, 3 KCl, 2 CaCl₂, 1 MgCl₂, 25 NaHCO₃, 1.25 NaH₂PO₄ and 25 glucose bubbled with carbogen and maintained at 35 ± 2 °C (Warner Instruments TC-324B). For whole-cell current clamp recordings 6–10 M Ω borosilicate glass patch electrodes (Harvard apparatus GC150F-15, 1.5 mm outer diameter \times 0.86 inner diameter, SDR scientific, Australia) were filled with an internal solution comprising

(mM) 135 potassium gluconate, 10 HEPES, 7 NaCl, 2 Na₂ATP, 0.3 Na₃GTP, 2 MgCl₂.

Slices were visualized at 40 \times magnification under bright field and infrared differential interference contrast video microscopy (Olympus BX51-WI). Somatic recordings were made using a Multiclamp 700B (Axon Instruments) and digitized with a Digidata 1440A, under the control of Axograph (Axograph X 1.5.4) and data acquired at a sampling rate of 50 kHz.

Whole-cell current clamp recordings were conducted on layer 5 (L5) pyramidal neurons. As we hypothesized *a priori* that stimulation would alter neuronal excitability and membrane properties, whole-cell recordings were made without applying holding currents during experimental procedures.

To investigate action potential (AP) properties (AP threshold, spike rise time, spike height, fast after hyperpolarization), single AP's were evoked with a 5-ms long depolarizing current step of +800 pA (Fig. 1D), repeated every second for a total of 10 s (i.e. 10 single AP's per recording).

To investigate the spike firing properties, spikes were evoked with an AP family protocol (Fig. 1C) consisting of 500-ms current steps ranging from -200 to $+500$ pA (20 current steps, with a 30-second interstep interval), which was repeated once more after a 30-s delay.

Cells were discarded and excluded from analysis if the series resistance changed by $> 20\%$ of baseline value and/or exceeded 30 M Ω . Current clamp bridge balance was adjusted prior to each AP family and single AP recording.

Repetitive magnetic stimulation (LI-rMS)

The LI-rMS protocol delivered was iTBS (Huang et al., 2005) (Fig. 1B) and consisted of trains of three 50-Hz pulses, repeated every 200 ms for 2 s. Trains were repeated once every 10 s for a total of 20 repetitions (total of 190 s). Monophasic pulses (400 μ s rise time) were delivered with a custom circular coil (described in (Tang et al., 2016) (8 mm outer diameter, with an iron core). Coils were fixed to an electronic micro-manipulator and positioned in-between the slice chamber and microscope condenser (Fig. 1A). The coil was placed at a distance of approximately 1 mm from the slice, with the coil edge placed below the cortical layers; therefore apical dendrites from layer 5 pyramidal neurons were oriented perpendicular to the coil. The peak magnetic field at a distance of 1 mm from the base of the coil was measured with a Hall-effect probe (Honeywell, SS94A2D, USA) to be 85.4 mT and had a dB/dT of ~ 285 T/s. Coils were controlled by an arbitrary waveform generator (Agilent 33551B, Measurement innovation, Australia) and a programmable DC power supply (Kepco BOP 100-4 M, TMG test equipment, Australia). Sham stimulation consisted of placing a coil detached from the power supply beneath the slice as described above for 190 s before beginning the post-stimulation₊₀ recordings.

Data analysis

Three single AP traces at each time point were analyzed for (i) AP threshold (change in membrane potential at a

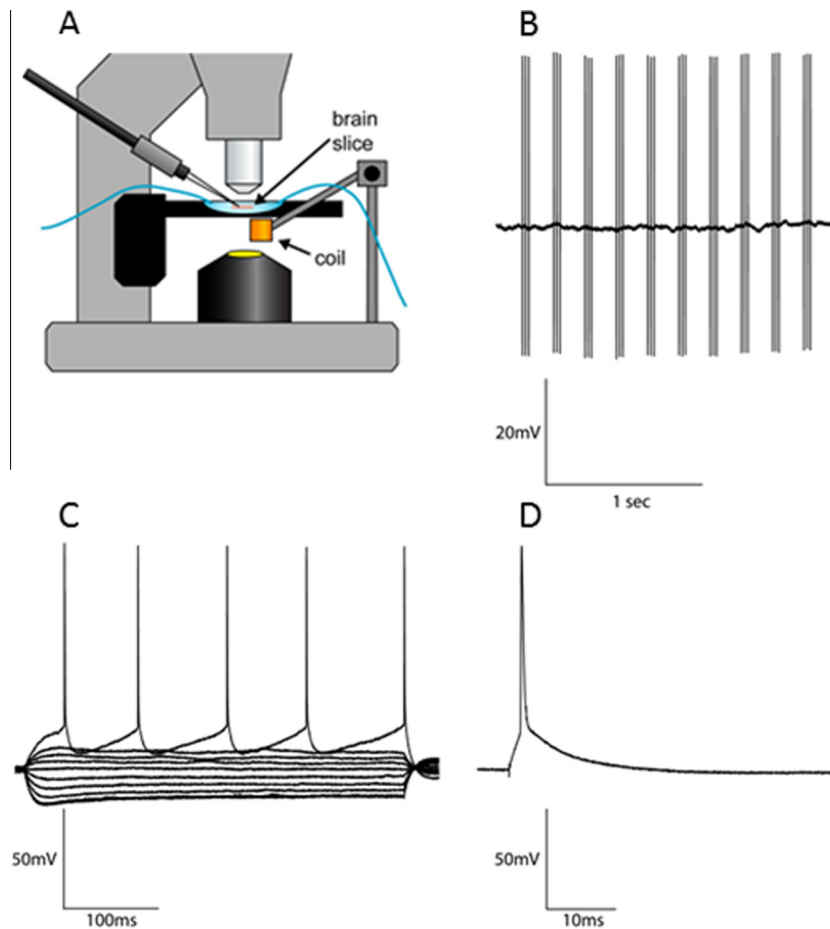


Fig. 1. *In vitro* LI-rMS delivery setup and representative traces of evoked spiking. LI-rMS was delivered with a custom 8 mm LI-rMS coil attached to a motorized head stage placed below slice chamber (A). Membrane potential recording during iTBS (B). Spike trains (C), and single AP's (D) evoked with electrical stimulation.

171 rate of 50 V/s) (ii) Spike height above resting membrane
172 potential (iii) 20–80% rise time of spike peak (iv) spike
173 half-width and (v) peak fast after hyperpolarization
174 (AHP). AP family recordings were analyzed for (i)
175 average resting membrane potential (RMP) (ii) rheobase
176 (lowest current step that induced 1 or more APs), (iii)
177 input resistance (iv) spike frequency. For spike
178 frequency analysis, the number of spikes evoked by the
179 500-ms depolarizing current steps was quantified.

180 To confirm that LI-rMS did not trigger action potential
181 firing with direct activation or through inducing
182 suprathreshold currents in the electrode wire (Mueller
183 et al., 2014; Pashut et al., 2014), we analyzed the mem-
184 brane potential recorded during LI-rMS. There was no evi-
185 dence of membrane after hyperpolarization following
186 single or trains of LI-rMS pulses in any of the traces. Fur-
187 thermore, the stimulus artifact had a peak voltage of
188 $58.02 \text{ mV} \pm 0.07$ relative to the resting membrane poten-
189 tial, which is below the mean action potential spike height
190 ($\sim 110 \text{ mV}$), suggesting that LI-rMS did not induce action
191 potential firing.

192 Statistical analysis

193 Statistical analysis was completed with IBM SPSS
194 statistics 20 and data graphed with Graphpad Prism 6.

195 Only cells contributing data for each of the 4 time points
196 were included in the analysis. Initial analyses were
197 completed on the raw values and confirmed that there
198 were no significant differences in the baseline values
199 between iTBS and sham for all the outcome measures.
200 Further analysis on the raw values showed that
201 although the mean baseline values were not significantly
202 different, small differences in the baseline means
203 obscured the detection of significant differences when
204 running *post-hoc* tests. Therefore, we analyzed the data
205 using an internal control method where the data at each
206 of the post-stimulation time points was expressed as a
207 *change relative to baseline for that cell* to account for
208 any small differences in the baseline means between
209 groups.

210 Normality was verified with Q–Q plots and
211 homogeneity of variance tested with Levene's test.
212 Data were analyzed with repeated measures
213 ANOVAs. Degrees of freedom were corrected with
214 Greenhouse-Geisser estimates when the
215 assumptions of sphericity were violated (Mauchly's
216 test). *Post-hoc* testing was performed using Sidak-
217 corrected multiple comparisons tests and *p* values
218 less than 0.05 were considered statistically
219 significant. All data are represented as mean
220 \pm standard error of the mean.

RESULTS

LI-rMS induces a hyperpolarized AP threshold and increases spike firing frequency

LI-rMS induced a more hyperpolarized AP threshold (Fig. 2A) relative to sham stimulation ($F_{1, 17} = 4.52, p = 0.048$). LI-rMS reduced the mean AP threshold by $1.76 \text{ mV} \pm 1.13$ (post-stimulation₊₀), $0.77 \text{ mV} \pm 1.10$ (post-stimulation₊₁₀) and $2.08 \text{ mV} \pm 1.60$ (post-stimulation₊₂₀). Post-hoc analysis showed a significant AP threshold hyperpolarization with LI-rMS at post-stimulation₊₀ ($p = 0.025$) and post-stimulation₊₂₀ ($p = 0.045$). There was no significant interaction between time and stimulation ($F_{2, 34} = 2.70, p = 0.082$).

Similarly, LI-rMS increased evoked spike firing frequency relative to sham stimulation ($F_{1,238} = 14.813, p = 0.001$) (Fig. 2B). LI-rMS increased the mean spike-firing frequency by $1.74 \text{ Hz} \pm 0.32$ (post-stimulation₊₀), $3.33 \text{ Hz} \pm 0.54$ (post-stimulation₊₁₀) and $4.44 \text{ Hz} \pm 0.61$ (post-stimulation₊₂₀) (Fig. 2C–E). Post-hoc analysis showed a significant increase in spike firing induced by LI-rMS at post-stimulation₊₀ ($F_{1,264} = 20.681, p = 0.001$) post-stimulation₊₁₀ ($F_{1,264} = 18.781, p = 0.001$) and

post-stimulation₊₂₀ ($F_{1, 264} = 5.683, p = 0.018$). There was no significant effect of current step amplitude ($F_{13,138} = 1.603, p = 0.085$) or significant interactions between time and stimulation ($F_{1,486, 353.746} = 3.359, p = 0.068$) or stimulation and current step amplitude ($F_{1, 13} = 0.503, p = 0.922$).

LI-rMS does not alter passive membrane properties, spike shape properties or fast after-hyperpolarization

In contrast to AP threshold and spike firing frequency, LI-rMS did not significantly change RMP ($F_{1, 17} = 0.56, p = 0.46$), rheobase ($F_{1, 17} = 1.02, p = 0.328$), spike height ($F_{1, 17} = 0.54, p = 0.473$), spike rise time ($F_{1, 17} = 0.001, p = 0.983$), spike half width ($F_{1, 17} = 2.320, p = 0.146$) or fast AHP ($F_{1, 17} = 0.848, p = 0.370$) (Fig. 3).

LI-rMS did not alter the input resistance (Fig. 3B) ($F_{1, 17} = 0.50, p = 0.49$) and was similar to sham for the first 10 min post-stimulation but trended toward a difference at 20 min post-stimulation. However, follow up analysis of the input resistance showed no significant differences in input resistance between sham and LI-rMS at post-

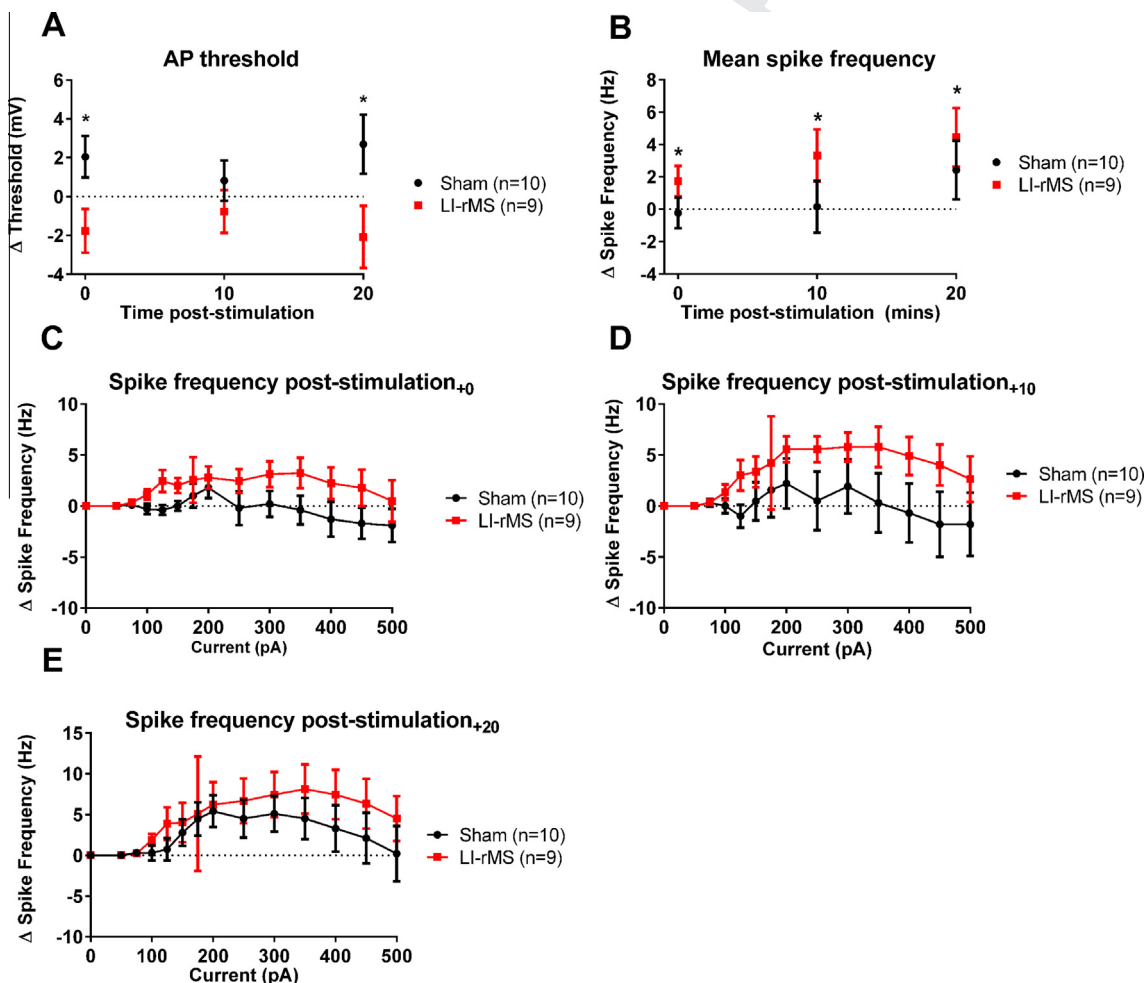


Fig. 2. LI-rMS alters AP threshold and spike firing frequency. LI-rMS significantly hyperpolarized the AP threshold (A) and increased spike firing frequency (B). Changes in spike frequency as function of current step amplitude at post-stimulation₊₀ (C), post-stimulation₊₁₀ (D), post-stimulation₊₂₀ (E). * $p < 0.05$, error bars represent SEM.

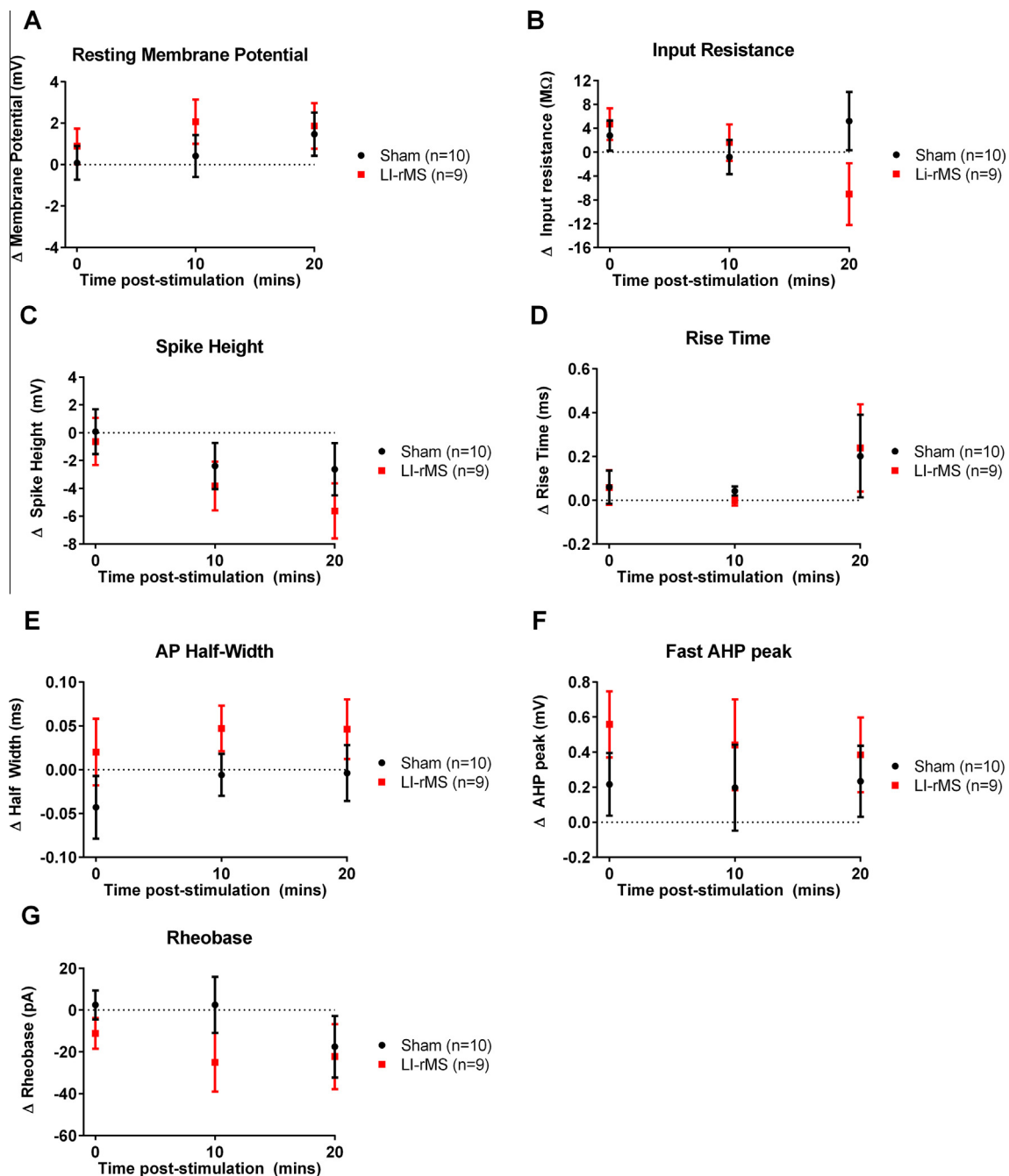


Fig. 3. LI-rMS does not alter passive membrane properties, AP shape or the rheobase. LI-rMS does not alter RMP (A), input resistance (B), spike height (C), AP rise time (D), AP half width (E), fast AHP (F) or rheobase (G) ($p > 0.05$). Error bars represent SEM.

264 stimulation₊₀ ($p = 0.608$), post-stimulation₊₁₀
265 ($p = 0.572$) and post-stimulation₊₂₀ ($p = 0.106$).

DISCUSSION

267 To our knowledge, this is the first study to investigate the
268 acute effects of LI-rMS at the single-cell level in cortical
269 excitatory neurons. The main findings of our study show
270 that LI-rMS does not alter passive membrane properties
271 (RMP and input resistance) but increases neuronal
272 excitability by inducing a more hyperpolarized AP

273 threshold and increased evoked spike firing frequency
274 relative to sham stimulation. Changes in AP threshold
275 were present immediately after and 20 min post-
276 stimulation whereas spike frequency changes were
277 found immediately after stimulation and persisted to
278 20 min post-stimulation.

279 Given that the RMP remained unchanged, a
280 hyperpolarized AP threshold is evidence of an LI-rMS-
281 induced increase in neuronal excitability, due to
282 modulation of membrane potential mechanisms at
283 depolarized levels. Mechanisms affecting AP threshold/

AP initiation include changes in fiber thickness and in the density and properties of voltage-gated sodium channels (Stuart et al., 1997; Kole et al., 2008). However, the changes in AP threshold were observed immediately after stimulation (190 s after onset), and changes in fiber thickness and the density of voltage-gated sodium channels (VGSCs) are unlikely to have occurred within such a short timeframe. Moreover, high-intensity rMS-induced structural changes, including changes in receptor density, have previously been shown to take greater than two hours post-stimulation (Vlachos et al., 2012). Rather, it is more likely that LI-rMS-induced changes in the properties of VGSCs, and has been suggested previously for voltage-gated calcium channels (for a review see reference (Pall, 2013)). Such a mechanism may underlie the change in AP threshold, probably through a direct modulation of the voltage-sensing mechanism, resulting in the opening of the VGSCs at more hyperpolarized voltages. Interestingly, the changes in AP threshold were present immediately and at 20 min post-stimulation but were not at 10 min post-stimulation. The apparent cyclical nature of AP threshold hyperpolarization may be due to LI-rMS altering the voltage-sensing mechanism by two different pathways, each with different times of onset. The immediate AP threshold hyperpolarization may be due to a direct interaction with LI-rMS (e.g. with the induced electric field during stimulation) whereas the AP threshold hyperpolarization 20 min post-stimulation may be due to activation of a biochemical/signaling pathway with a longer onset. As LI-rMS has previously been shown to increase intracellular calcium release in cortical neurons (Grehl et al., 2015), one such pathway that may underlie the longer onset change to AP threshold is through calcium signaling/calmodulin which is known to alter VGSC function (Herzog et al., 2003).

Our second line of evidence that LI-rMS increases neuronal excitability is the increase in evoked spike firing following stimulation. Multiple channels are known to regulate spike firing frequency through alterations in the after hyperpolarization that follows spike firing (Hille, 2001), including A-type potassium channels (K_A) for L5 pyramidal neurons (Kang et al., 2000) which may have been modulated by LI-rMS. Interestingly, analysis of our single AP data revealed no change in the peak fast AHP accompanying the significant increases in spike firing frequency (see Fig. 3F). The involvement of K_A channels varies between single and repetitive firing, with a greater role of K_A channels during repetitive firing (Kang et al., 2000). Therefore LI-rMS-induced increases in spike frequency may be due to modulation of specific K_A channel properties, which would require separate pharmacological investigation.

Since LI-rMS lowered the AP threshold, we expected to observe a concurrent reduction in the rheobase current. While the mean rheobase current decreased over time following LI-rMS, it did not reach statistical significance. It is possible that our increments in current steps (25-pA steps in the 50–200-pA range) may have been too large to detect subtle changes in rheobase (i.e. changes < 25 pA) underlying a reduction in AP threshold of ~2 mV.

Our results are in part, similar to a recent study using high-intensity rTMS (Hoppenrath et al., 2016). The authors also show that rTMS increases neuronal excitability, with increased spike frequency in fast-spiking interneurons when probed at two hours post-stimulation. Interestingly the authors also found changes to the resting membrane potential. Therefore it is possible that LI-rTMS and rTMS share common effects (e.g. changes in spike frequency) with high-intensity rTMS capable of more profound effects (e.g. altered resting membrane) due to increased intensity.

Recordings of the membrane potential during LI-rMS confirmed that the delivered stimulation intensity did not directly induce AP firing (i.e. subthreshold stimulation). In contrast to high-intensity rTMS where stimulation is believed to result in neuronal firing through trans-synaptic (Labedi et al., 2014; Lenz et al., 2016) or direct activation (Lenz et al., 2016). Therefore our results provide further evidence that subthreshold stimulation induced by LI-rMS is capable of modulating neural plasticity. These results are in line with previous studies from our laboratory that used 12 mT rTMS in mice (approximately 2 orders of magnitude lower than suprathreshold rTMS) to induce structural and molecular plasticity (Rodger et al., 2012; Makowiecki et al., 2014). Although we provide evidence that LI-rMS modulates certain electrophysiological properties of cortical pyramidal neurons, further studies are needed to determine whether LI-rMS-induced plasticity is neuron subtype specific (e.g. pyramidal vs interneurons) or brain region specific (e.g. cerebellum (Morellini et al., 2014) vs hippocampus etc.) as well as whether non-neuronal cells such as glia (Cullen and Young, 2016) can be modulated.

It is well established that the endogenous electrophysiological properties of pyramidal neurons differ between young and adult animals (Zhang, 2004; Etherington and Williams, 2011). In our study, we used slices from developing mice (12–15 days post-natal) whereas previous high-intensity rMS studies have mostly used adult animals (~3 months old) to demonstrate plasticity of both inhibitory and excitatory networks using electrophysiological (Hsieh et al., 2014; Thimm and Funke, 2015) and molecular methods (Trippe et al., 2009; Hoppenrath and Funke, 2013). Interestingly, the recent study by Hoppenrath et al. showed a significant age effect on high-intensity rMS-induced plasticity in fast-spiking interneurons, with increases in evoked spike firing frequency present in young adult animals (post-natal days 29–38) but absent in juvenile (post-natal days 26–28) and older adult animals (post-natal days 40–62) (Hoppenrath et al., 2016). In contrast, our results show LI-rMS alters the excitability properties (including evoked spike firing frequency) in motor and somatosensory slices from developing animals (post-natal days 12–15). At this age, pyramidal neurons are in a heightened state of plasticity as they are approaching the end of the critical periods for both motor and somatosensory systems (Hensch, 2004). The intrinsic properties of the developing neurons, including their heightened plasticity state, may affect the capacity of LI-rMS to induce plasticity and the mechanism whereby it does so. Therefore, future studies

406 in older animals are needed to determine whether the
407 changes observed in developing tissue also occur in adult
408 tissue. However, we have previously shown that LI-rTMS
409 increases corticospinal excitability in anaesthetized adult
410 rats, providing evidence of LI-rTMS-induced plasticity in
411 adult animals (Tang et al., 2016).

412 We have provided insight into the acute effects of LI-
413 rMS on single excitatory cortical neurons. Our results
414 show that LI-rMS increases excitability of L5 pyramidal
415 neurons from motor and somatosensory brain slices, by
416 modulating specific active and spiking properties without
417 altering passive membrane properties. These results
418 further our understanding of LI-rMS-induced plasticity
419 and highlight the capability of subthreshold magnetic
420 stimulation to induce functional plasticity.

421 *Acknowledgments—The authors would like to thank Mr. Marty*
422 *Firth for statistical advice (School of Mathematics and Statistics*
423 *UWA) and E/Professor Donald Robertson (Auditory Lab, UWA)*
424 *for useful discussions regarding membrane modulation. This*
425 *work was funded by the Neurotrauma Research Program of*
426 *Western Australia awarded to AG and JR. JR was supported*
427 *by a National Health and Medical Research Council of Australia*
428 *senior research fellowship (APP1002258). JNJR was supported*
429 *by a Rutherford Discovery Fellowship from the Royal Society of*
430 *NZ. LJB was supported by a Neurological Foundation of NZ Miller*
431 *Scholarship. ADT was supported by an Australian Postgraduate*
432 *Award, the University of Western Australia and the Bruce and*
433 *Betty Green Foundation.*

434 REFERENCES

435 Capone F, Dileone M, Profice P, Pilato F, Musumeci G, Minicuci G,
436 Ranieri F, Cadossi R, Setti S, Tonali P, Di Lazzaro V (2009) Does
437 exposure to extremely low frequency magnetic fields produce
438 functional changes in human brain? *J Neural Transm*
439 116:257–265.
440 Cullen CL, Young KM (2016) How does transcranial magnetic
441 stimulation influence glial cells in the central nervous system?
442 *Front Neural Circuits* 10:26.
443 Di Lazzaro V, Capone F, Apollonio F, Borea PA, Cadossi R, Fassina
444 L, Grassi C, Liberti M, Paffi A, Parazzini M (2013) A consensus
445 panel review of central nervous system effects of the exposure to
446 low-intensity extremely low-frequency magnetic fields. *Brain*
447 Stimul 6:469–476.
448 Etherington SJ, Williams SR (2011) Postnatal development of
449 intrinsic and synaptic properties transforms signaling in the layer
450 5 excitatory neural network of the visual cortex. *J Neurosci*
451 31:9526–9537.
452 Grehl S, Viola H, Fuller-Carter PI, Carter KW, Dunlop SA, Hool L,
453 Sherrard RM, Rodger J (2015) Cellular and molecular changes to
454 cortical neurons following low intensity repetitive magnetic
455 stimulation at different frequencies. *Brain Stimul* 8:114–123.
456 Hensch TK (2004) Critical period regulation. *Annu Rev Neurosci*
457 27:549–579.
458 Herzog RI, Liu C, Waxman SG, Cummins TR (2003) Calmodulin
459 binds to the C terminus of sodium channels Nav1.4 and Nav1.6
460 and differentially modulates their functional properties. *J Neurosci*
461 23:8261–8270.
462 Hille B (2001) Ion channels of excitable membranes. MA: Sinauer
463 Sunderland.
464 Hoppenrath K, Funke K (2013) Time-course of changes in neuronal
465 activity markers following iTBS-TMS of the rat neocortex.
466 *Neurosci Lett* 536:19–23.
467 Hoppenrath K, Härtig W, Funke K (2016) Intermittent theta-burst
468 transcranial magnetic stimulation alters electrical properties of

fast-spiking neocortical interneurons in an age-dependent 469
fashion. *Front Neural Circuits* 10:22. 470
Hsieh T-H, Huang Y-Z, Rotenberg A, Pascual-Leone A, Chiang Y-H, 471
Wang J-Y, Chen J-J (2014) Functional dopaminergic neurons in 472
substantia nigra are required for transcranial magnetic 473
stimulation-induced motor plasticity. *Cereb Cortex*. 474
Huang Y-Z, Edwards MJ, Rounis E, Bhatia KP, Rothwell JC (2005) 475
Theta burst stimulation of the human motor cortex. *Neuron* 476
45:201–206. 477
Kang J, Huguenard JR, Prince DA (2000) Voltage-gated potassium 478
channels activated during action potentials in layer V neocortical 479
pyramidal neurons. *J Neurophysiol* 83:70–80. 480
Kole MH, Ilshner SU, Kampa BM, Williams SR, Ruben PC, Stuart 481
GJ (2008) Action potential generation requires a high sodium 482
channel density in the axon initial segment. *Nat Neurosci* 483
11:178–186. 484
Labeledi A, Benali A, Mix A, Neubacher U, Funke K (2014) Modulation 485
of inhibitory activity markers by intermittent theta-burst stimulation 486
in rat cortex is NMDA-receptor dependent. *Brain Stimul* 487
7:394–400. 488
Lenz M, Galanis C, Muller-Dahlhaus F, Opitz A, Wierenga CJ, Szabo 489
G, Ziemann U, Deller T, Funke K, Vlachos A (2016) Repetitive 490
magnetic stimulation induces plasticity of inhibitory synapses. *Nat* 491
Commun 7:10020. 492
Makowiecki K, Harvey A, Sherrard R, Rodger J (2014) Low-intensity 493
repetitive transcranial magnetic stimulation improves abnormal 494
visual cortical circuit topography and upregulates BDNF in mice. *J* 495
Neurosci 34:10780–10792. 496
Morellini N, Grehl S, Tang A, Rodger J, Mariani J, Lohof AM, Sherrard 497
RM (2014) What does low-intensity rTMS do to the cerebellum? 498
Cerebellum 14:23–26. 499
Mueller JK, Grigsby EM, Prevosto V, Petraglia Iii FW, Rao H, Deng Z- 500
D, Peterchev AV, Sommer MA, Egnor T, Platt ML, Grill WM 501
(2014) Simultaneous transcranial magnetic stimulation and 502
single-neuron recording in alert non-human primates. *Nat* 503
Neurosci 17:1130–1136. 504
Müller-Dahlhaus F, Vlachos A (2013) Unraveling the cellular and 505
molecular mechanisms of repetitive magnetic stimulation. *Front* 506
Mol Neurosci 6:50. 507
Pall ML (2013) Electromagnetic fields act via activation of voltage- 508
gated calcium channels to produce beneficial or adverse effects. *J* 509
Cell Mol Med 17:958–965. 510
Pashut T, Magidov D, Ben-Porat H, Wolfus S, Friedman A, Perel E, 511
Lavidor M, Bar-Gad I, Yeshurun Y, Korngreen A (2014) Patch- 512
clamp recordings of rat neurons from acute brain slices of the 513
somatosensory cortex during magnetic stimulation. *Front Cell* 514
Neurosci 8. 515
Ridding MC, Rothwell JC (2007) Is there a future for therapeutic use 516
of transcranial magnetic stimulation? *Nat Rev Neurosci* 517
8:559–567. 518
Rodger J, Mo C, Wilks T, Dunlop SA, Sherrard RM (2012) 519
Transcranial pulsed magnetic field stimulation facilitates 520
reorganization of abnormal neural circuits and corrects 521
behavioral deficits without disrupting normal connectivity. 522
FASEB J 26:1593–1606. 523
Stuart G, Spruston N, Sakmann B, Häusser M (1997) Action potential 524
initiation and backpropagation in neurons of the mammalian CNS. 525
Trends Neurosci 20:125–131. 526
Tang A, Thickbroom G, Rodger J (2015) Repetitive transcranial 527
magnetic stimulation of the brain: mechanisms from animal and 528
experimental models. *Neuroscientist*. [http://dx.doi.org/10.1177/](http://dx.doi.org/10.1177/1073858415618897) 529
[1073858415618897](http://dx.doi.org/10.1177/1073858415618897). 530
Tang AD, Lowe AS, Garrett AR, Woodward R, Bennett W, Carty AJ, 531
Garry MI, Hinder MR, Summers JJ, Gersner R, Rotenberg A, 532
Thickbroom G, Walton J, Rodger J (2016) Construction and 533
evaluation of rodent-specific rTMS coils. *Front Neural Circuits* 10. 534
<http://dx.doi.org/10.3389/fncir.2016.00047>. 535
Thimm A, Funke K (2015) Multiple blocks of intermittent and 536
continuous theta-burst stimulation applied via transcranial 537
magnetic stimulation differently affect sensory responses in rat 538
barrel cortex. *J Physiol* 593:967–985. 539

540 Trippe J, Mix A, Aydin Abidin S, Funke K, Benali A (2009) Theta burst
541 and conventional low-frequency rTMS differentially affect
542 GABAergic neurotransmission in the rat cortex. *Exp Brain Res*
543 199:411–421. 551
544 Vlachos A, Muller Dahlhaus F, Rosskopp J, Lenz M, Ziemann U,
545 Deller T (2012) Repetitive magnetic stimulation induces functional
546 and structural plasticity of excitatory postsynapses in mouse
547 organotypic hippocampal slice cultures. *J Neurosci*
548 32:17514–17523. 552
549 Wagner T, Rushmore J, Eden U, Valero-Cabre A (2009) Biophysical
550 foundations underlying TMS: setting the stage for an effective use
551 of neurostimulation in the cognitive neurosciences. *Cortex*
552 45:1025–1034. 553
554 Wischnewski M, Schutter DJ (2015) Efficacy and time course of theta
555 burst stimulation in healthy humans. *Brain Stimul* 8:685–692. 554
556 Z-w Zhang (2004) Maturation of layer V pyramidal neurons in the rat
557 prefrontal cortex: intrinsic properties and synaptic function. *J*
558 *Neurophysiol* 91:1171–1182. 555
559 Ziemann U, Paulus W, Nitsche MA, Pascual-Leone A, Byblow WD,
560 Berardelli A, Siebner HR, Classen J, Cohen LG, Rothwell JC
561 (2008) Consensus: motor cortex plasticity protocols. *Brain Stimul*
562 1:164–182. 556
563
564

(Accepted 17 August 2016)
(Available online xxxx)

UNCORRECTED PROOF